Interaction between Laser-Produced Plasma and Guiding Magnetic Field

Jun Hasegawa, Kazumasa Takahashi, Shunsuke Ikeda, Mitsuo Nakajima, and Kazuhiko Horioka

Department of Energy Sciences, Tokyo Institute of Technology, Yokohama 226-8502, Japan

ABSTRACT

Transportation properties of laser-produced plasma through a guiding magnetic field were examined. A drifting dense plasma produced by a KrF laser was injected into an axisymmetric magnetic field induced by permanent ring magnets. The plasma ion flux in the guiding magnetic field was measured by a Faraday cup at various distances from the laser target. Numerical analyses based on a collective focusing model were performed to simulate plasma particle trajectories and then compared with the experimental results.

Keywords

Laser-produced plasma, high-current ion source, guiding magnetic field, plasma transportation, collective effect

1. Introduction

Since the invention of laser in early 1960s, dense plasma generated by high-power laser irradiation of solid material has been recognized as a potential source of highly stripped ions, leading to numerous studies on laser ion sources for particle accelerators [1,2]. As one of the pioneering works, Phaneuf reported the generation of Fe^{16+} and C^{6+} by a CO_2 laser with a power density of $\sim 10^{10}$ W/cm^2 [3]. Luther-Davies *et al.* revealed that when the laser power density reached $\sim 10^{15}$ W/cm^2, considerably high charged ions such as Au^{38+} were produced with MeV kinetic energies [4].

Besides the production of highly charged ions, the laser-produced plasma has the potential to supply high-flux, low-emittance ion beams owing to its large drift velocity perpendicular to the laser-irradiated solid surface. Barabash *et al.* recognized this feature of the laser-produce plasma and examined the applicability of the laser ion source to heavy ion fusion (HIF) injectors [5]. They produced low charged ions Pb^+ and Pb^{2+} by irradiating a lead target with a CO_2 laser. Hasegawa, *et al.* also generated a low temperature, dense plasma composed mainly of Cu^+ and Cu^{2+} by using a Nd:YAG laser with a power density slightly above an ablation threshold for copper ($\sim 10^8$ W/cm^2) and showed that it meets a demand for the ion flux from HIF driver accelerators.

To achieve high power densities above the ablation thresholds with relatively small laser energies ($\leq$ 1 J), the laser pulse must be shorter than ~1 μs. However, beam pulse lengths longer than 1-10 μs are frequently required to increase the accelerator duty cycle or relax strong space charge repelling forces. To achieve long pulse beam extraction, the laser ion source usually has a long drift space where the plasma freely expands toward the extraction gap [8]. Since ions in the laser-produce plasma have not only large drift velocity but also large momentum spread, a plasma pulse duration larger than ~10 μs is easily achieved by plasma expansion over several meters.

On the other hand, since the laser-produced plasma expands three-dimensionally during the drift, its flux rapidly drops with the drift distance. To suppress the flux decrease, Gray *et al.* applied an axial magnetic field to the drift space and confined the plasma

transversely [9]. They observed the enhancement of highly charged ions as well as the total plasma ion flux. Okamura *et al.* also have recently tested the confinement of a laser-produced plasma using a solenoid magnetic field and succeeded in extending the plasma pulse duration with suppressing the flux decrease [10].

The KEK digital accelerator facility is now planning to replace the present ECR ion source by a laser ion source and adopt a plasma-guiding scheme using a permanent magnet array instead of a solenoid. The use of the permanent magnet is preferable from the engineering viewpoint because it allows us to eliminate the power supply to the high-voltage terminal for the excitation and cooling of the solenoid.

In this study, we investigated both experimentally and numerically the transportation of a laser-produced plasma drifting through a guiding magnetic field induced by coaxially arranged ring magnets. From the viewpoint of ion source engineering, the purpose of this study is to find periodic magnetic field profiles, with which efficient plasma transportation is achieved. In addition, the interaction process between an expanding laser-produced plasma and an axial magnetic field is very complex because the time scale of magnetic field diffusion into the plasma is almost comparable to that of plasma expansion. This fact also motivates us to conduct this study from the viewpoint of plasma physics.

2. Experimental Setup

Figure 1 shows a schematic of the experimental setup. A copper target, whose surface was mirror polished by fine alumina particles (~0.3 μm), was set in a vacuum of 10^{-4} Pa. A KrF excimer laser irradiated the target with an incidence angle of ~70° and produced a dense plasma plume. The energy and duration of the laser pulse were, respectively, ~120 mJ and ~20 ns. The laser spot on the target surface was a rectangle of 0.5×1.5 mm^2, resulting in a power density of ~8×10^8 W/cm^2.

The laser-produced plasma rapidly expands into vacuum with a large center-of-mass velocity perpendicular to the target surface. Then the plasma plume was guided into a drift tube by an axial magnetic field. The guiding magnetic field was induced by permanent ring magnets, which were coaxially arranged along the tube with equal intervals. Each ring magnet has an inner diameter of 60 mm, an outer diameter of 120 mm, and a thickness of 20 mm. By changing the magnet interval d from 0 to 40 mm, we examined the effect of the field profile on the plasma transportation. The distance from the laser target to the entrance of the magnet array was fixed to be 350 mm throughout this study.

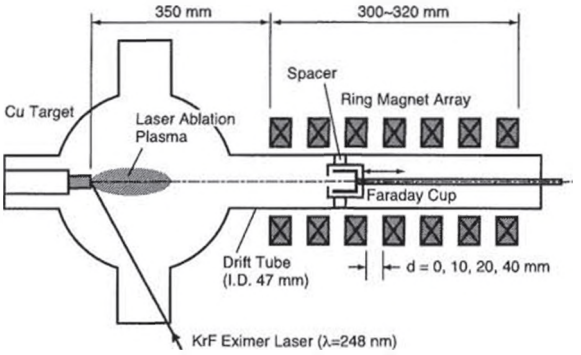

Fig. 1. A schematic of experimental setup.

Figure 2 shows axial magnetic field profiles $B_z(z)$ on the center axis of the drift tube calculated by the Poisson-Superfish code [11]. Note that the magnetic field quickly changes its polarity near the entrance ($L \sim 350$ mm) and exit ($L \sim 650$ mm) of the magnet array owing to cusp-like field structures. This reversal of the field is the most remarkable when

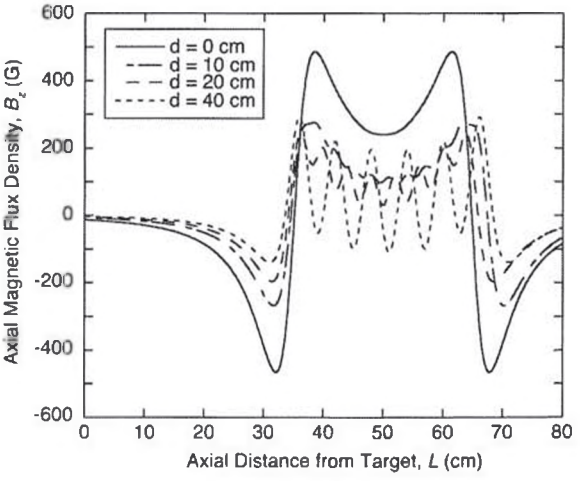

Fig. 2. Magnetic field profiles on drift tube axis.

$d = 0$. Meanwhile, when $d \neq 0$, ripples appear on the field profiles. The amplitude of the ripple becomes larger with magnet interval.

We used a Faraday cup with a secondary electron suppressor to measure the plasma ion flux. The cup was supported by a linear motion feed through having a stroke of 400 mm, enabling us to set the cup at any positions in the drift tube. An insulator spacer was inserted between the cup cage and the drift tube wall so that the entrance aperture of the cup (ø6 mm) could be always located exactly on the center axis of the tube. The cup and the suppressor were biased to –400 V and –300 V, respectively. Before recoding a plasma flux waveform by a digital oscilloscope, we cleaned up the copper target surface by several laser shots in advance to minimize the effect of impurities on the current waveform.

3. Numerical Analysis

3.1 Fundamental equations

To analyze the behavior of a drifting plasma injected into an axial magnetic field, we adopted the collective focusing model proposed by Robertson [12]. Kraft *et al.* showed that this model well predict the behavior of a neutralized high-current pulsed ion beam in a solenoidal magnetic field [13].

Here we assume that the laser-produced plasma drifts along the center axis of the guiding magnet field and the perturbation of the field induced by the plasma is small enough to be ignored. In addition, the plasma neutrality is assumed to hold always.

The Lagrangian for a charge particle moving a magnetic field is given by:

$$L = \tfrac{1}{2} m\mathbf{v}^2 + q\mathbf{v}\cdot\mathbf{A} - q\phi . \tag{1}$$

Here, m, q, and $\mathbf{v}$ are, respectively, the mass, charge, and velocity of the particle. $\mathbf{A}$ and ϕ are, respectively, the vector and scalar potentials of the field. The canonical momentum of the particle is derived from Eq. (1):

$$\frac{\partial L}{\partial \dot{\theta}} = P_\theta = mr^2 \frac{d\theta}{dt} + qrA_\theta . \tag{2}$$

If we assume that the plasma particle has no momentum in the azimuthal direction when it is produced (t = 0), the conservation of the canonical momentum requires that $P_\theta = 0$ hold throughout the particle motion. Then, Eq. (2) gives:

$$\frac{d\theta}{dt} = -qA_\theta / mr . \tag{3}$$

By applying Eq. (3) to the Lagrange equation for radial direction, we obtain the equation of motion for the plasma particle:

$$\frac{d^2 r}{dt^2} = -\frac{q^2}{m^2} A_\theta \frac{\partial A_\theta}{\partial r} + \frac{qE_r}{m} . \tag{4}$$

When we assume $r_i(t) = r_e(t)$ as a plasma quasi-neutrality condition, $dr_i^2(t)/dt^2 = dr_e^2(t)/dt^2$ is satisfied throughout the particle motion, where the subscripts i and e denote ion and electron, respectively. By applying this relationship to Eq. (4) and solving it for the axial electric field E_r, we obtain:

$$E_r = \frac{q_i m_e + q_e m_i}{m_e m_i} A_\theta \frac{\partial A_\theta}{\partial r} . \tag{5}$$

By substituting E_r in Eq. (4) by Eq. (5), the equation of motion for the plasma particle finally becomes:

$$\frac{d^2 r}{dt^2} - \frac{q_e q_i}{m_e m_i} A_\theta \frac{\partial A_\theta}{\partial r} = 0 . \tag{6}$$

Eq. (6) means that ions and electrons in the plasma behave as if they were particles having a charge of $(q_e q_i)^{1/2}$ and a mass of $(m_e m_i)^{1/2}$. The electric field and the equation of motion for the axial direction are also derived by the same procedure:

$$E_z = \frac{q_i m_e + q_e m_i}{m_e m_i} A_\theta \frac{\partial A_\theta}{\partial z} , \tag{7}$$

$$\frac{d^2 z}{dt^2} - \frac{q_e q_i}{m_e m_i} A_\theta \frac{\partial A_\theta}{\partial z} = 0 . \tag{8}$$

Eq. (6) and (8) determine the orbit of the plasma particle in an axisymmetric magnetic field.

3.2 Numerical simulation

To calculate plasma particle orbits in an axial magnetic field using Eqs. (6) and (8), we used the azimuthal component of the vector potential A_θ obtained by interpolating the field data output from the Poisson-Superfish code (Fig. 2). The 4th-order

Runge-Kutta method was employed for the time integration of the equations of motion.

In this study, the simulation assumed that all plasma particles are emitted from the center of the copper target ($z = r = 0$) at $t = 0$ because both the laser pulse (~10 ns) and the laser spot (~0.5 mm) are negligibly small compared with the temporal and spatial scales of the plasma expansion (~10 μs, ~100 mm), respectively.

The plasma particles are assumed to have a drift-Maxwellian velocity distribution given by:

$$f(v_r, v_z) = n\left(\frac{m}{2\pi kT}\right)^{3/2} \exp\left(-mv_r^2/2kT\right) \times \exp\left(-m(v_z - v_d)^2/2kT\right), \quad (9)$$

where n is the plasma number density, T is the plasma temperature, and v_d is the axial drift velocity. The temperature and the drift velocity were determined by fitting a measured plasma-ion-flux waveform by a TOF (time of flight) distribution function derived from Eq. (9):

$$f_{TOF}(t) = Ct^{-4} \exp\left(-m(L/t - v_d)^2/2kT\right). \quad (10)$$

The simulation iteratively calculated the orbits of the plasma particles (typically for 100 test particles) with randomly changing initial velocities based on the above distribution function.

3. Results and Discussion

Figure 3 shows a typical plasma ion flux (solid line) observed 350 mm downstream from the copper target when no guiding magnetic field was applied. The reproducibility of the waveform was very high and the shot-to-shot fluctuation of the peak height was less than a few percent.

The dashed line in the figure is the result of a curve fit by Eq. (10), which gives $v_d \approx 7.6\times10^3$ m/s and $T \approx 56$ eV. Note that this T value indicates only that the plasma particles have a large momentum spread because the rapidly expanding laser-produced plasma is considered not in an equilibrium state defined by a single temperature value. We consider that this large momentum spread was induced principally in the hydrodynamic acceleration process in the early stage of the plasma expansion. The experiments in this

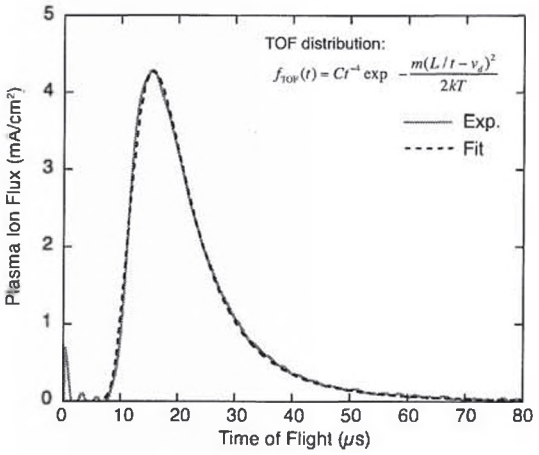

Fig. 3. Typical waveform of plasma ion flux without guiding magnetic field.

study were conducted under a fixed laser irradiation condition, so we used the above values as initial parameters for numerical simulations.

Typical current waveforms of the plasma ion flux measured in a guiding magnetic field ($d = 0$ mm) are shown in Fig. 4. To check the reproducibility, two or three waveforms taken at the same condition are superimposed. One can see that the plasma ion flux is enhanced several times compared with the case without the guiding field. In addition, ripples appear on the waveforms, which degrades the reproducibility. We found that this tendency became more remarkable with increasing magnet interval.

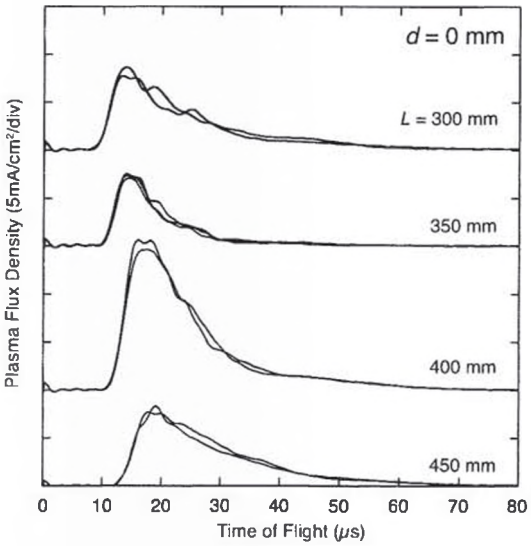

Fig. 4. Typical waveform of plasma ion flux with guiding magnetic field.

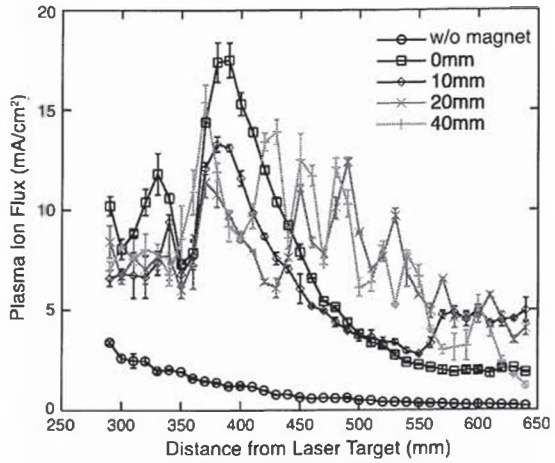

Fig. 5. Dependence of peak ion-current density on plasma drift distance.

The peak value of the plasma ion flux was plotted as a function of drift distance from the target in Fig. 5. The figure compares the cases with a guiding magnetic field (d = 0, 10, 20, and 40 mm) to the case without the field. The plasma ion flux increases by a factor of ~2 even before the plasma enters the magnet array (L < 350 mm). We consider that this enhancement is attributed to the transverse compression of the plasma by the converging magnetic field near the entrance of the magnet array. When d = 0 mm and 10 mm, the plasma ion flux drastically increases immediately after the plasma passes through the cusp-like field region (L ~ 350 mm) and reaches the maximum at L ~ 400 mm. Then the flux decreases gradually with drift distance.

For larger magnet intervals (d = 20 mm and 40 mm), the plasma behavior becomes more complex. Although the overall tendencies are similar to those for smaller interval cases, the plasma ion flux largely fluctuates even at the middle part of the magnet array (L = 400~600 mm). This result implies that the plasma transportation was very sensitive to the perturbation of the guiding magnet field.

Figure 6 plots the calculated trajectories of the plasma particles in the guiding magnetic field. Since the trajectories of 100 test particles are overlaid, the figure shows not an instantaneous spatial plasma distribution but the envelope of the drifting plasma. The maximum initial divergence angle of the plasma

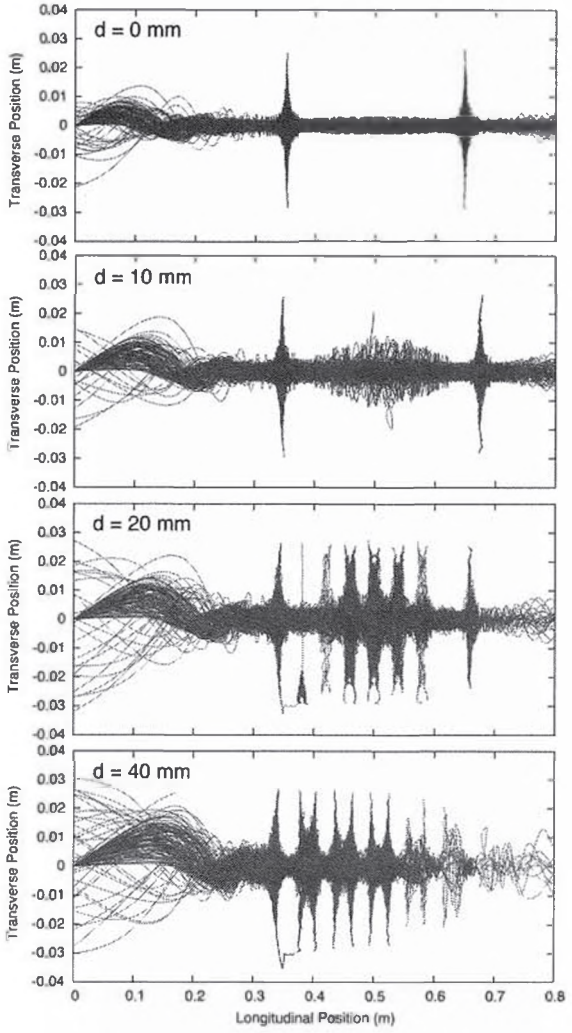

Fig. 6. Trajectories of plasma particles in guiding magnetic fields.

particle was defined to be θ_{max} = $\tan^{-1}(24/120) \sim 11.3°$ from the drift tube radius (~24 mm) and the distance from the target to the entrance of the drift tube (~120 mm). The initial divergence angle was randomly changed from 0 to θ_{max} in this calculation by considering the axial symmetry of the magnetic field.

As shown in Fig. 6, the transverse compression of the plasma near the magnet array entrance (L ~ 300 mm) depends slightly on the magnet interval. When d = 0 mm, the plasma compression occurs most strongly, leading to the effective plasma collection. Meanwhile, the compression effect becomes weaker with increasing magnet interval, resulting in relatively larger plasma radius. The

number of reflected plasma particles also increases with magnet interval.

The unwanted effect of the reversal of the field at the array entrance is almost independent of the magnet interval. Since the field strength increases with increasing radial position in the permanent magnet array, plasma particles trapped by the cusp-like field cannot escape from it. Such particles are finally lost at the tube wall. The sudden drop in the observed plasma flux at L = 350 mm is probably due to the rapid plasma expansion by the cusp-like field. After passing through the cusp-like field, the plasma is compressed again and transported to the array exit as shown in Fig. 6. Particularly for d = 0 mm and 10 mm, the plasma transportation is relatively stable in the array. These results well explain experimentally observed plasma behaviors shown in Fig. 5.

On the other hand, when the magnet interval is equal to or larger than each ring magnet width (20 mm), the plasma transportation is largely influenced by the field fluctuations even inside the array. The plasma undergoes expansion and compression repeatedly and the particle loss in the expansion phase largely decreases the transportation efficiency. This result suggests that the magnet interval should be less than the width of the permanent magnet composing the array.

4. Concluding remarks

This study proposed to use a permanent magnet array to guide a laser-produced plasma and examined the feasibility of this plasma-guiding scheme by preliminary experiments and simple numerical simulations. In contrast to the solenoidal magnetic field, the magnetic field induced by the permanent magnet array intrinsically has cusp-like structures. We found that such a field structure led to a large plasma loss. However, by setting the magnet intervals to be smaller than the width of each permanent ring magnet, the plasma could be transported effectively. Particularly, the converging field structure near the magnet array entrance may increase the utilization ratio of the laser-produced plasma.

On the other hand, the application of the guiding magnetic field may increase the averaged transverse momentum of the plasma particle, which affects the emittance of the beam extracted from the plasma. This effect must be investigated more precisely. Fortunately, the collective focusing model seems to well reproduce the behavior of the plasma in the axial guiding magnetic field in the parameter regime treated in this study, probably enabling us to examine the emittance problem by using the simulation code employed in this study.

References

[1] C. De Michelis: "Laser interaction with solids - A bibliographical review", *IEEE J. Quant. Electronics*, QE-6, p.630 (1970).

[2] G. F. Tonon : "Laser Sources for Multiply-Charged Heavy Ions", *IEEE Trans. Nucl. Sci.*, NS-19, p.172 (1972).

[3] R. A. Phaneuf: "Production of High-Q Ions by Laser Bombardment Method", IEEE Trans. Ncul. Sci., NS-28, p.1182 (1981).

[4] B. Luther-Davies and J. L. Hughes, "Observations of MeV ions emitted from a laser produced plasma", Opt. Commun., vol. 18, pp. 351-353 (1976).

[5] L. Z. Barabash, D. G. Koshkarev, Y. I. Lapitskii, S. V. Latyshev, A. V. Shumshurov, Y. A. Bykovskii, A. A. Golvbev, Y. P. Kosyrev, K. I. Krechet, R. T. Haydarov, and B. Y. Sharkov: "Laser produced plasma as an ion source for heavy ion inertial fusion", *Laser Part. Beams*, 2, p.49 (1984).

[6] J. Hasegawa, M. Yoshida, Y. Oguri, M. Ogawa, M. Nakajima, and K. Horioka: "High-current laser ion source for induction accelerators", *Nucl. Instr. and Meth. B* 161-163, pp. 1104-1107 (2000).

[7] M. Yoshida, J. Hasegawa, J. W. Kwan, Y. Oguri, M. Nakajima, K. Horioka, and M. Ogawa: "Grid-Controlled Extraction of Low-Charged Ions from a Laser Ion Source," *Japan. J. Appl. Phys.*, Vol. 42, pp. 5367-5371

(2003).

[8] B. Y. Sharkov, S. Kondrashev, I. Roudskoy, S. Savin, A. Shumshurov, H. Haseroth, et al.: "Laser ion source for heavy ion synchrotrons", Rev. Sci. Instrum., Vol. 69, pp. 1035-1039 (1998).

[9] L. G. Gray, R. H. Hughes, and R. J. Anderson: "Heavy ion source using a laser generated plasma transported through an axial magnetic field", J. Appl. Phys., 53, 6628 (1982).

[10] M. Okamura, A. Adeyemi, T. Kanesue, J. Tamura, K. Kondo, and R. Dabrowski: "Magnetic plasma confinement for laser ion source", Rev Sci Instrum, Vol. 81, p. 02A510 (2010).

[11] http://laacg.lanl.gov/laacg/services/serv_codes.phtml

[12] S. Robertson: "Collective focusing of an intense ion beam", Phys. Rev. Lett. Vol. 48, No. 3, 149 (1982).

[13] R. Kraft, B. Kusse, and J. Moschella: "Collective focusing of an intense pulsed ion beam", Phys. Fluids, Vol. 30, 245 (1987).